Techno-Economic Evaluation on Solar-Assisted Post-Combustion CO_2 Capture in Hollow Fiber Membrane Contactors

Junkun Mu , Jinpeng Bi , Yuexia Lv * , Yancai Su , Wei Zhao , Hui Zhang , Tingting Du , Fuzhao Li , Hongyang Zhou

Posted Date: 9 April 2024

doi: 10.20944/preprints202404.0550.v1

Keywords: solar thermal energy; membrane gas absorption; hollow fiber membrane contactor; technical feasibility; economic assessment

Article

Techno-Economic Evaluation on Solar-Assisted Post-Combustion CO_2 Capture in Hollow Fiber Membrane Contactors

Junkun Mu [1,2], Jinpeng Bi [1,2], Yuexia Lv [1,2,*], Yancai Su [1,2], Wei Zhao [1,2], Hui Zhang [1,2], Tingting Du [3,4], Fuzhao Li [1,2] and Hongyang Zhou [1,2]

[1] School of Mechanical Engineering, Qilu University of Technology (Shandong Academy of Sciences), Jinan 250353, China
[2] Shandong Institute of Mechanical Design and Research, Jinan 250031, China
[3] School of Energy and Power Engineering, Shandong University, Jinan 250061, China
[4] Shenzhen Research Institute of Shandong University, Shenzhen 518057, China
* Correspondence: yuexialv@foxmail.com

Abstract: Membrane gas absorption technology and solar-assisted regeneration system are two promising approaches to reduce high energy consumption associated with carbon dioxide capture from coal fired power plants. In the present study, a solar-assisted hollow fiber membrane contactor (SOL-HFMC) power plant is proposed to capture and desorb CO_2 in hollow fiber membrane contactors with the assistance of solar thermal collectors. Techno-economic assessment and sensitivity analysis of the proposed system is carried out in three studied locations with different weather conditions for a 580 MWe pulverized coal power plant. Research results show that, the output capacity and net efficiency of the SOL-HFMC power plant are significantly higher than those of the reference power plant regardless whether TES system is applied or not. In addition, CEI of the SOL-HFMC power plant with TES system is 4.36 kg CO_2/MWh, 4.45 kg CO_2/MWh and 4.66 kg CO_2/MWh lower than that of the reference power plant. The prices of membrane, vacuum tube collector and phase change material should be reduced to achieve lower LCOE and COR values. Specifically for SOL-HFMC power plant with TES system, the corresponding vacuum tube collector price shall be lower than 25.70 \$/m^2 for Jinan, 95.20 \$/m^2 for Xining, and 128.70 \$/m^2 for Lhasa, respectively. To be more competitive than solar-assisted ammonia-based post-combustion CO_2 capture power plant, the membrane price in Jinan, Xining and Lhasa shall be reduced to 0.012 \$/m, 0.015 \$/m and 0.016 \$/m for the sake of LCOE, and 0.03 \$/m, 0.033 \$/m and 0.034 \$/m for the sake of COR, respectively. The findings can provide guidance for decision-making and risk management strategies.

Keywords: solar thermal energy; membrane gas absorption; hollow fiber membrane contactor; technical feasibility; economic assessment

1. Introduction

Global warming due to increasing concentrations of greenhouse gases in the atmosphere has resulted in profound and detrimental effects on our planet, such as sea level rise, extreme weather events, and disruptions to ecosystems and biodiversity. The Intergovernmental Panel on Climate Change (IPCC) highlighted that, the rise in global average temperature shall be limited to 1.5°C above the preindustrial level to achieve the ambitions of the Paris Agreement [1]. The European Union and the US White House both have the ambitious targets of achieving net-zero greenhouse gas emissions by 2050 [2]. Similarly, China has announced its commitment to peak its carbon dioxide emissions before 2030 and attain carbon neutrality by 2060[3]. Transitioning to sustainable renewable energy, improving energy efficiency, and carbon capture and storage (CCS) have been considered as three

 doi:10.20944/preprints202404.0550.v1

effective approaches to reduce greenhouse gas emissions and global average temperature rise [4]. CCS is an attractive strategy to stabilize or reduce atmospheric CO_2 levels in the short term, which involves the CO_2 capture from industrial processes, transportation from large scale emission sources via ship or in a pipeline, and final storage in deep underground geological formations.

CO_2 post-combustion capture system is promising to mitigate CO_2 emissions from coal-fired power plants due to its applicability to existing power plants and industrial facilities without major modifications. The most well-established chemical absorption technology is facing the high regeneration costs and operation problems such as flooding, absorbent losses, entrainment, liquid channeling and foaming. Furthermore, the solvent is generally regenerated via the thermal energy extracted from steam turbine cycles proposes extra energy consumption, resulting in a dramatic drop of 20-25% in the electricity production during power generation [5]. Therefore, a variety of efforts have been made to reduce the heavy energy penalty associated with solvent regeneration process [6–9].

In the past two decades, membrane gas absorption technology has been attracting more and more attentions as an energy-efficient and cost-effective alternative because it combines the advantages of high selectivity from chemical absorption and compact design from membrane separation. Membrane gas absorption technology offers several advantages, including high efficiency, low energy consumption, compact system design, and scalability, which has been extensively utilized in various industries such as power plants, refineries, and manufacturing facilities to reduce greenhouse gas emissions [10,11]. For a studied 685 MWe coal-fired power plant, the energy consumption and capital cost of CO_2 capture in hollow fiber membrane contactors were reduced by 43% and 31% compared with packed bed columns, respectively [12]. An energy saving of 4.83% and a capital cost reduction of 6.11% can be achieved by such as membrane-absorption hybrid CO_2 capture process compared to a stand-alone absorption process [13]. In comparison with traditional desorber columns, the hollow fiber membrane contactors can reduce the energy duty for desorbing CO_2 by half, from 4 MJ/kg CO_2 to 2 MJ/kg CO_2, indicating that membrane gas absorption technology is a promising alternative approach to regenerate CO_2-rich absorbent [14].

In parallel, the utilization of renewable solar energy has also emerged as a sustainable solution to reduce the reliance on thermal energy from the power plant during the CO_2 regeneration stage to avoid a significant reduction in power generation efficiency. Correspondingly, numerous studies have been carried out to investigate the technical and economic feasibility of such integration methods [15,16]. To overcome the major drawback of intermittent supply of renewable solar energy, the solar-assisted regeneration system is generally coupled with thermal energy storage (TES) system [17]. The idea of integrating solar thermal concentrators into CO_2 capture process from the flue gas of a 300 MW_e power plant for solvent regeneration was firstly proposed in New South Wales, Australia [18]. Liu et al. [19]evaluated the influences of types of solar thermal collector involved in ammonia-based solar-assisted post-combustion carbon capture (PCC) in three typical locations in China. They concluded that vacuum tube collector (VTC) was more attractive than parabolic trough collector in the studied cases, and calculated the critical collector prices to achieve lower levelized costs of electricity (LCOE) and cost of CO_2 removed (COR) than those of the traditional PCC system. More recently, Khalilpour et al. [20] presented a novel solvent regeneration system by replacing the complex desorber column with a parabolic trough pipe to eliminate steam generation process, which reduced the capital expenditure by approximately 15-30% and increased the operation flexibility of power plant with PCC process. The life cycle impact assessment for solar thermal integration in post-combustion carbon capture showed that, the levelized global warming potential per unit of electricity production for the 100% solar-powered PCC is the lowest in comparison with conventional PCC and solar-assisted PCC at a solar fraction of 23%. Thus, it has a global warming reduction of 38.1% for the 330 MWe and 18.1% for the 660 MWe power-plants, respectively [21]. Obviously, the integration of solar thermal energy offers a promising pathway towards achieving more environmentally friendly and economically feasible carbon capture solutions.

As previously mentioned, membrane gas absorption technology and solar-assisted absorbent regeneration are two promising approaches to reduce the associated energy penalty and even achieve

 doi:10.20944/preprints202404.0550.v1

sustainability of CO_2 post-combustion capture process. By integrating these two technologies, there is potential to achieve more CO_2 elimination with lower energy requirements, thereby addressing the challenges of climate change and reducing the environmental impact of carbon emissions. However, up to now, there is no literature reported on the technical feasibility and application potential of integrating membrane gas absorption technology and solar-assisted regeneration method for post-combustion carbon capture. Correspondingly, it is the interest of the present study to design a novel system to utilize the solar thermal energy to provide heat for CO_2 capture in hollow fiber membrane contactors, named as solar-assisted hollow fiber membrane contactor (SOL-HFMC) system. The reference power plant absorbs and desorbs CO_2 in hollow fiber membrane contactors by 100% extracted steam is called STE-HFMC power plant. Three locations in China with different solar radiation conditions have been selected as the study cases to investigate the technical potential of the proposed SOL-HFMC system. Furthermore, the Total capital requirement (TCR), levelized cost of electricity (LCOE) and cost of CO_2 removed (COR) are calculated to explore the economic performance of the proposed SOL-HFMC system. Finally, sensitivity analysis is carried out to assess the impact of changes in key parameters on the performance and cost-effectiveness of the proposed system, to provide guidance for decision-making and risk management strategies.

2. System Description

The schematic drawing of the solar assisted CO_2 capture system using hollow fiber membrane contactors in a coal fired power plant is shown in Figure 1. The SOL-HFMC power plant is composed of three main parts: a coal fired power plant, a solar thermal energy collection and storage system, a membrane contactor based CO_2 absorption-desorption system.

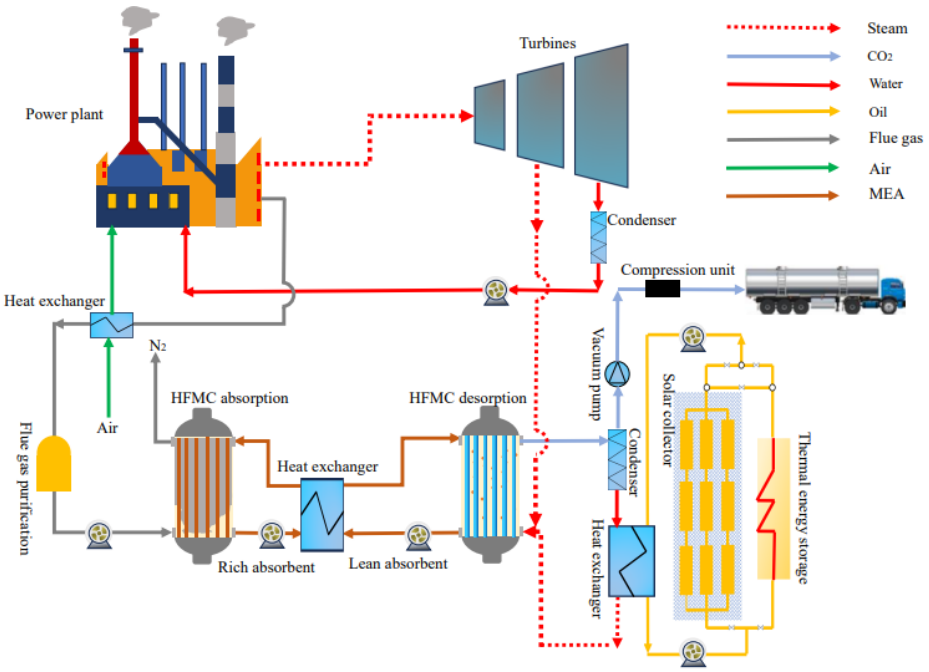

Figure 1. Schematic drawing of the proposed SOL-HFMC power plant.

2.1. Membrane Contactor Based CO2 Absorption-Desorption System

In this paper, the 580 MWe power plant is selected according to The NETL Baseline Studies for Fossil Energy Plants [22]. 20 wt. % monoethanolamine (MEA) is used as the absorbent due to its advantages of high absorption capacity, low volatility and regeneration energy, easy availability and cost-effectiveness [23]. Specific to the membrane material, the polypropylene (PP) membrane is selected in this study attributed to its high void volume, wide commercial size, cost effectiveness, high chemical stability, and thermal stability [24]. The flue gas emitted from the power plant firstly passes through a heat exchanger chilled by air to reduce the gas temperature, and further pretreated

 doi:10.20944/preprints202404.0550.v1

with desulfurization and dust removal processes before entering the hollow fiber membrane contactor. The main composition of the purified flue gas is mainly N_2 and CO_2.

In the CO_2 absorption process, the flue gas and the absorbent flow in counter-current directions on the shell side and tube side of the hydrophobic PP membrane contactor, respectively. Driven by concentration gradients, the CO_2 in the flue gas diffuses through the micropores of the membrane wall to the gas-liquid interface and is absorbed into the liquid phase by MEA solution. Meanwhile, the hydrophobic PP membrane material prevents the MEA solution from entering the gas phase, thereby achieving the separation of CO_2 from flue gas. Unlike traditional gas separation membrane based on pore size sieving, and dissolution-diffusion separation mechanisms, the microporous hollow fiber membrane material used in membrane gas absorption technology does not provide selectivity for the gas to be separated. It serves only as the interface between the gas and liquid phases, with selectivity provided by the liquid phase MEA solution, achieving gas separation through a diffusion-absorption mechanism. The exhaust gas after eliminating CO_2, is mainly N_2 to be emitted directly into the atmosphere.

The rich absorbent containing the absorbed CO_2 is brought to the heat exchanger and then pumped into other hollow fiber membrane contactors for further desorption. The rich absorbent flows in the lumen side and counter-currently contacts the sweeping steam supplied from the bottom. The regenerated lean absorbent is pumped from the bottom of the desorption unit and circulated back to the absorption membrane contactors for the continuous absorption cycle. The CO_2 extracted from the top of the desorption unit is condensed in a condenser to remove the water vapor, and the released CO_2 can be captured for storage or further utilization. To guarantee the long-time operation stability of PP membrane and minimize the regeneration energy consumption of rich absorbent, the regeneration process is maintained at the temperature of 80℃ and the pressure of 30 kPa [25].

2.2. Solar Thermal Energy Collection and Storage System

As shown in Figure 1, the thermal energy required for regenerating CO_2-rich absorbent is primarily provided by solar thermal energy, and supplemented by the steam extracted from the turbine in case of insufficient solar radiation. In this study, the desorption temperature of the CO_2-rich absorbent is set at 80 ℃, and thus the low-temperature range of solar thermal collectors with the range of 50-150 ℃ are applied. Under the condition of meeting desorption temperature requirement, the solar radiation is collected by vacuum tube collectors due to its advantages of lower cost and easier maintenance in comparison with other types of solar thermal collectors [26].The vacuum tube collector absorbs sunlight through its surface and heat the working fluid inside the collector. The heated working fluid achieves thermal energy transfer to condenser water to generate low-pressure steam through the heat exchanger, and then pumped back to vacuum tube collector for process recycle. Thermal oil is used as the working fluid in the collector to prevent the solar collector from operating under high pressure. To eliminate the intermittence and instability feature of solar energy, a TES system is also designed according to the principle given by Mokhtar et al. [27], in order to achieve stable and efficient and operation of solar thermal utilization systems. Erythritol is selected as the phase change material (PCM) for thermal management because of excellent superior phase-transition properties.

3. Methodology and Study Case

This section may be divided by subheadings. It should provide a concise and precise description of the experimental results, their interpretation, as well as the experimental conclusions that can be drawn.

3.1. Net Efficiency and Carbon Emission of Coal-Fired Power Plants

It is assumed that the studied power plant works continuously for 24 hours every day with an idle month for maintenance in August. The parameters of hollow fiber membrane contactor are

 doi:10.20944/preprints202404.0550.v1

identical with reference [12]. The detailed parameters of the power plant without and with CCS are shown in Table 1.

Table 1. Performance parameters of the power plant.

Technical parameters	Value	References
Baseline power plant without CCS		
Auxiliary load (MWe)	30	[22]
Net output power (MWe)	550	[22]
Coal consumption (kg/h)	185759	[22]
CO_2 emission (t/h)	441	[22]
CO_2 concentration of flue gas (% mol)	13.53	[22]
STE-HFMC power plant		
Number of HFMC	200	[12]
HFMC diameter (m)	2.8	[12]
HFMC effective height (m)	4.0	[12]
HFMC total height (m)	4.2	[12]
Chemical absorbent	MEA	
Absorbent mass fraction (wt. %)	20	
Regeneration energy consumption (MJ_{th}/kg CO_2)	1.25	[25]
CO_2 capture rate (%)	90	
Purity of desorbed CO_2 (%)	98	
Absorption temperature (K)	300	
Regeneration temperature (K)	353	
Blower and pump power (MWe)	5	[12]
Vacuum pump power (MWe)	26	[12]
Compression power (MWe)	38	[12]
Capacity reduction due to steam extraction (MWe)	24	
Power output after CO_2 capture (MWe)	457	

It is assumed that the studied power plant works continuously for 24 hours every day with an idle month for maintenance in August. The parameters of hollow fiber membrane contactor are identical with reference [12]. The detailed parameters of the power plant without and with CCS are shown in Table 1.

Due to the steam extracted from the steam turbine for CO_2-rich absorbent regeneration, the integration of CO_2 capture unit with coal-fired power plant results in the work loss of steam turbine and net efficiency reduction of the power plant. The corresponding work loss per unit mass of desorbed CO_2 of the steam turbine W_{lost} (MJ_e/kg_{CO2}) can be calculated by the following equation:

$$W_{lost} = Q_{th} \times \alpha = Q_{th} \times \left(1 - \frac{T_{abs}}{T_{reg} + \Delta T}\right) \quad (1)$$

where Q_{th} is the thermal energy required for per unit mass of CO_2 desorption (MJ_{th}/kg_{CO2}); α is the steam equivalent coefficient (MJ_e/MJ_{th}); T_{abs} is the absorption temperature (K), taking 300K in this study; T_{reg} is the CO_2-rich absorbent regeneration temperature (K), taking 353 K in this study; T_{tur} is the temperature of the steam extracted from the gas turbine (K), and is assumed to be 363 K in this study; ΔT is the temperature difference between the extracted steam and CO_2-rich absorbent regeneration temperature, K.

 doi:10.20944/preprints202404.0550.v1

When solar thermal energy collection and storage system is applied for absorbent regeneration, solar thermal energy can be used to replace partial steam extracted from the power plant, which can reduce the power loss of gas turbine and improve the net electricity generation of power plant. The net output capacity of the plant integrated with SOL-HFMC system can be expressed by the following equation:

$$P_{SOL-HFMC} = P_{STE-HFMC} + P_{solar} \quad (2)$$

where $P_{SOL-HFMC}$ is the net output capacity of the SOL-HFMC power plant, MW_e; $P_{STE-HFMC}$ is the net output capacity of the STE-HFMC power plant, MW_e; P_{solar} is the incremented net output capacity due to existence of solar thermal energy collection and storage system, MW_e.

Thus, the net efficiency of the SOL-HFMC power plant can be improved in compared with that of the STE-HFMC power plant, which can be calculated by the following equation:

$$\eta_{SOL-HFMC} = \frac{P_{SOL-HFMC}}{m_{fuel} \times LHV} \quad (3)$$

where m_{fuel} is the fuel mass consumption flow, kg/h; LHV is the low heating value of the fuel, kJ/kg fuel.

Carbon emission intensity (CEI, MWh/kgCO_2) typically refers to the amount of CO_2 emitted to atmosphere per unit of electricity generated, which can be used to evaluate the design of the SOL-HFMC system from the perspective of greenhouse gas emission. CEI is calculated by Equation 4:

$$CEI = \frac{CO_{2,out}}{Electricity_{out}} \quad (4)$$

where $CO_{2,out}$ is the CO_2 emitted from the power plant with different CO_2 capture systems, kg; $Electricity_{out}$ is the net output electricity of the power plant with different CO_2 capture systems, MWh.

3.2.Area of Solar Thermal Collectors

To maximize the utilization of solar energy, the vacuum tube collector is installed facing south and its tilt angle is approximately equivalent to the location latitude [28]. The solar irradiation intensity varies with the climatic weather conditions. When the vacuum tube collectors are designed based on the highest monthly collected solar thermal energy divided by monthly sunshine hours thorough the year, the thermal energy harvested by the solar collectors during other months with lower solar irradiation is less than the regeneration energy demand during sunshine time. Under this condition, all harvest thermal energy is utilized to meet regeneration energy demand of CO_2-rich absorbent during sunshine time, and TES system is deactivated because there is no residual heat for further storage. In this study, for SOL-HFMC system without TES, the collector area corresponding to the highest value of monthly collected solar thermal energy divided by monthly sunshine hours is defined as Critical Area 1. On the other hand, the vacuum tube collectors can also be designed based on the lowest value of monthly collected solar thermal energy divided by monthly sunshine hours. In this case, the thermal energy harvested by the solar collectors during other months with higher solar irradiation is more than the regeneration energy demand during sunshine time, and surplus thermal energy is wasted. The corresponding collector area in this case is defined as Critical Area 2 in this study.

The thermal energy harvested by vacuum tube collectors Q (kWh) can be calculated by the following equation:

$$Q = G \times S \times \eta_{solar} \quad (5)$$

where G is the global horizontal radiation, kWh/m^2; S is the area of vacuum tube collectors, m^2; η_{solar} is the efficiency of vacuum tube collectors, which can be calculated by Equation 6:

$$\eta_{solar} = \alpha_0 - \alpha_1 \times \frac{(T_c - T_a)}{G} - \alpha_2 \times \frac{(T_c - T_a)^2}{G} \quad (6)$$

 doi:10.20944/preprints202404.0550.v1

where T_c is the temperature of the working fluid in the collector, K; T_a is the ambient temperature, K; α_0, α_1, α_2 are the optical efficiency parameters of the vacuum tube collector, taking α_0=0.71, α_1=0.5 W/m²/K, α_2=0.0035 W/m²/K², respectively [29].

Solar load fraction (SF) refers to the proportion of heat provided by solar energy to the total energy consumption required for regeneration of CO_2-rich absorbent, which is used to specifically quantify the extent to which solar energy contributes to meeting overall regeneration energy demands. A higher SF indicates greater reliance on renewable energy sources and reduced dependence on steam extracted from gas turbine of power plant for CO_2 regeneration. Mathematically, the SF for CO_2-rich absorbent regeneration can be expressed by:

$$SF = \frac{Q_{solar}}{Q_t} \tag{7}$$

where Q_{solar} is the energy provided by solar source, kWh; Q_t is total energy required for CO_2 regeneration, kWh.

3.3.Economic Evaluation Indicators

Undoubtedly, the integration of solar thermal collection and storage system will increase the investment costs of the CO_2 post-combustion capture system. The economic parameters of the of studied SOL-HFMC power plant are listed in Table 2.

Table 2. Economic parameters of the studied system.

Economic parameters	Value	References
Service lifespan of the project (years)	30	
Discount rate (%)	7	[30]
Power plant total equipment cost (M$)	444.7	[22]
Membrane contactor cost (M$)	76.2	[12]
Heat Exchanger (M$)	8.3	[12]
Pumps, blowers, coolers (M$)	10.7	[12]
Compression unit (M$)	50.1	[12]
Fuel cost (M$/year)	58.2	[22]
MEA replenishment (kg/t CO_2)	1.5	[5]
Vacuum tube collector price (USD/m²)	130	[19]
Energy storage material density (kJ/kg)	339.8	[19]
Energy storage material price ($/kg)	3.5	[19]

TCR, LCOE and COR are calculated to investigate the economic performance of the proposed SOL-HFMC power plant. TCR for the studied SOL-HFMC system is the sum of TCR for the coal fired power plant without CCS, the HFMC capture unit, the solar energy collection and storage system. TCR for the vacuum tube collectors and thermal storage system can be estimated using the parameters listed in Table 2. TCR for the power plant without CCS and the HFMC capture unit are estimated according to the methodology proposed in references[12,31–33], with the detailed information presented in Table 3. Due to the new technology with limited data, higher project contingencies are applied for the HFMC capture unit in comparison with those for the power plant without CCS. It can be calculated that, TCR for the power plant without CCS system and the HFMC capture unit is 1491.9 M$ and 626.2 M$, respectively.

 doi:10.20944/preprints202404.0550.v1

Table 3. TCR Calculation method.

Capital cost items	Quantification
Process equipment cost	444.7M$ for power plant without CCS [22]
	145.3 M$ for HFMC capture unit [12]
Supporting facilities cost	10% of process equipment cost
Direct and indirect labor cost	50% of process equipment cost
Bare Erected Cost (BEC)	Sum of the above items
Engineering services cost	18% of BEC
Process contingencies	5% of BEC for power plant without CCS
	40% of BEC for HFMC capture unit
Project contingencies	15% of all above
Total Plant Cost (TPC)	BEC + Engineering services + Contingencies
Owner's costs	15% of TPC [33]
Total Overnight cost (TOC)	TPC + Owner's costs
Total Capital Requirement	1.289×TOC

Levelized cost of electricity, named LCOE, is an indicator which is frequently applied to assess the cost effectiveness of integrating CCS technology into the power generation process, which can be calculated by the following equation:

$$LCOE = \frac{(TCR) \cdot (FCF) + FOM}{Electricity_{out}} + VOM + Fuel \quad (8)$$

$$FCF = \frac{r(1+r)^t}{(1+r)^t - 1} \quad (9)$$

where *TCR* is the total capital requirement, $; *FCF* represents fixed change factor, which can be calculated by Equation 9; *FOM* is the fixed O&M costs, accounting for 3.5% of the TCR[33], $/MWh; *VOM* is the sum of MEA cost and fuel consumption cost, $/MWh; *Fuel* is the fuel cost, $/MWh; $Electricity_{out}$ is the annual net electricity generation of the power plant, MWh/year; *r* is the discount rate, % and *t* is the service lifespan of the power plant, year.

Cost of CO_2 avoidance represents the additional cost incurred by implementing CCS technology to reduce carbon emissions compared to the baseline power plant without CCS (baseline PP), which can be used to evaluate the economic feasibility of adopting CCS technology. COR can be expressed by the following equation:

$$COR = \frac{LCOE_{cap} - LCOE_{base}}{CEI_{base} - CEI_{cap}} \quad (10)$$

where $LCOE_{cap}$ is the LCOE of power plant with CCS, $/MWh; $LCOE_{base}$ is the LCOE of power plant without CCS, $/MWh; CEI_{base} is the carbon emission intensity of power plant without CCS, t/MWh; CEI_{cap} is the carbon emission intensity of power plant with CCS, t/MWh

3.4. Study Case

The thermal collection capacity of a specified vacuum tube collector highly depends on the solar radiation incident on the collector surface. With the purpose of assessing the technical feasibility and economic benefits of the proposed system, three locations with different solar irradiation intensities are considered in the present study, namely Lhasa (29.6° N, 91.1° E), Xining (36.7° N, 101.7° E) and Jinan (36.5° N, 116.8° E). The distribution of total solar radiation on the horizontal surface in China, as well as the detailed locations of three studied cases, is presented in Figure 2.

Preprints.org (www.preprints.org) | NOT PEER-REVIEWED | Posted: 9 April 2024 doi:10.20944/preprints202404.0550.v1

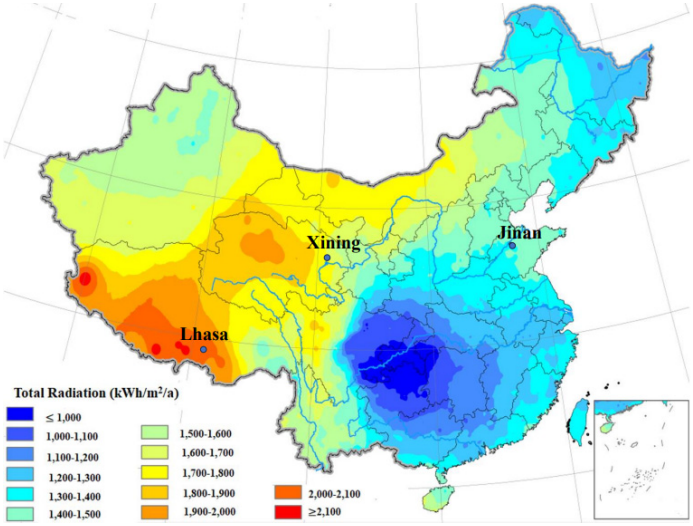

Figure 2. Solar radiation and location of three study cases.

The main meteorological parameters of the three studied cities were acquired from METEONORM Global Meteorological Database [34]. The monthly global horizontal radiation and monthly average sunshine hours of three studied cities are given in Figure 3. The annual global horizontal radiation in Lhasa, Xining and Jinan is 1988 kWh/m², 1578 kWh/m², and 1340 kWh/m² respectively. In Lhasa, the highest monthly global radiation is in June at 227 kWh/m², and the lowest is in February at 115 kWh/m². In Xining and Jinan, the highest radiation values are in May at 181 kWh/m² and 165 kWh/m² respectively, while the lowest values are in December at 74 kWh/m² and 56 kWh/m². Additionally, in terms of sunshine duration, the cities of Lhasa, Xining, and Jinan have the longest monthly sunshine durations of 280 hours, 261 hours, and 246 hours, respectively. The annual average ambient temperatures in Lhasa, Xining, and Jinan are 9.5°C, 6.4°C, and 14.9°C respectively.

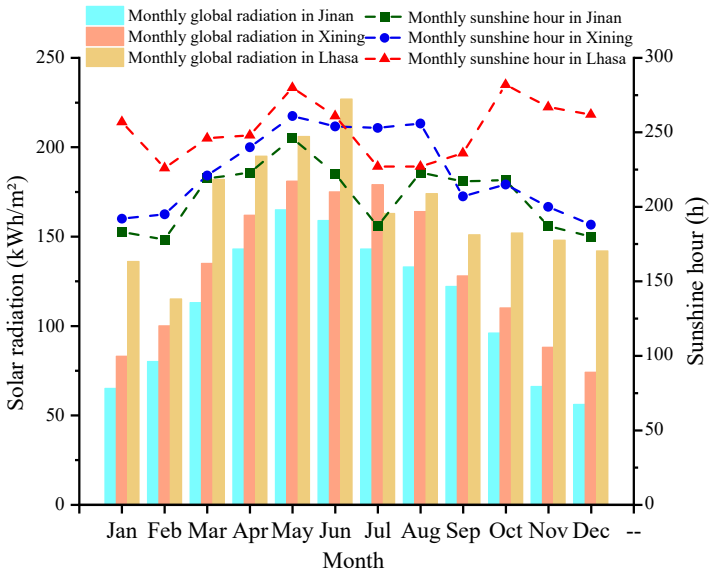

Figure 3. Main meteorological parameters in three cities.

4. Results and Discussion

4.1. Technical Feasibility Evaluatio

Authors should discuss the results and how they can be interpreted from the perspective of previous studies and of the working hypotheses. The findings and their implications should be discussed in the broadest context possible. Future research directions may also be highlighted.

 doi:10.20944/preprints202404.0550.v1

Figure 4 shows the monthly thermal energy collected by per unit area of vacuum tube collectors in three studied locations. To maximize the utilization of solar energy, the vacuum tube collectors are all installed towards the south, and the optimal tilt angle are set approximately equivalent to the location latitude, which is 30°, 37° and 36° for Lhasa, Xining and Jinan, respectively. It can be observed that, the maximum solar thermal energy can be obtained in Lhasa city due to the highest solar irradiation and the longest sunshine durations, following by Xining City and Jinan City.

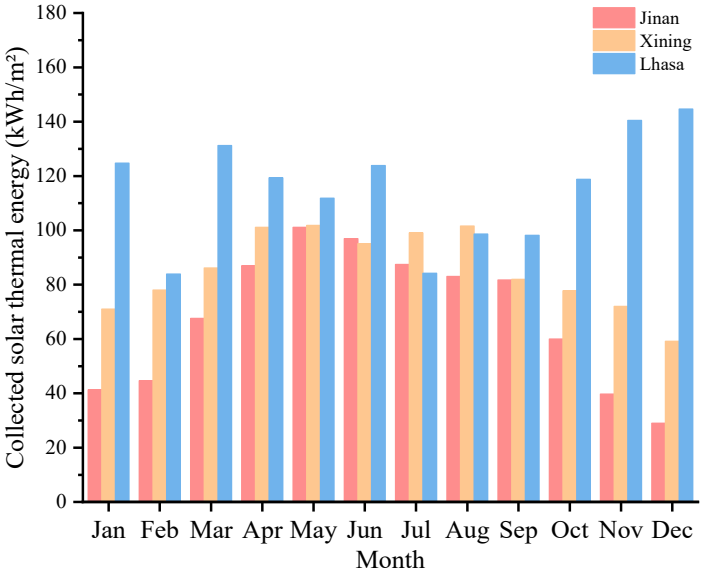

Figure 4. Monthly thermal energy harvested by the ETC at studied locations.

Authors should discuss the results and how they can be interpreted from the perspective of previous studies and of the working hypotheses. The findings and their implications should be discussed in the broadest context possible. Future research directions may also be highlighted.

TES system can be integrated with solar collectors to buffer the intermittency and fluctuation of solar energy resource for absorbent regeneration. Evidently, the TES capacity depends on the area of vacuum tube collectors. Figure 5 illustrates the relationship between thermal storage capacity and the solar load fraction. The required thermal storage capacity increases with an increase in solar load fraction. Specifically, the relationship is almost linear when the SF ranges are within 20-63%, 27-79% and 28-82% for Jinan, Xining and Lhasa, respectively. Within above specified ranges, the thermal storage capacity increases relatively slow with the increase in SF for all three studied cases. However, the required thermal storage capacity increases dramatically when the SF further increases beyond 63%, 79% and 82% for Jinan, Xining and Lhasa, respectively. Comprehensively considering the cost of PCM material and benefits of SF increase, the upper limit of thermal storage capacity is set at 15 Full Load Hours (FLH), which indicates that the TES system can support CO_2-rich absorbent regeneration energy demand for up to 15 hours. The minimum and maximum area of vacuum tube collectors required to meet the thermal storage capacity of 15FSH is defined as Critical Area 3 and Critical Area 4, respectively.

Figure 6 presents the calculation result of SF variations with the change of solar collector area. For SOL-HFMC system without TES system, the SF increases rapidly with the increase in solar collector area. When the solar collector area is increased beyond Critical Area 1, the SF still increases with the increase in solar collector area, but the increase rate of SF gradually decreases. When the solar collector area reaches Critical Area 2, the SF reaches its maximum value of 28.19%, 30.26% and 34.84% for Jinan, Xining and Lhasa cities, respectively. SF is stabilized at its maximum value even the solar collector area is further increased beyond Critical Area 2. The reason is that, the thermal energy supplied by solar collectors under Critical Area 2 is excessive for solvent regeneration during any sunshine hours, and surplus thermal energy is wasted due to absence of TES system.

 doi:10.20944/preprints202404.0550.v1

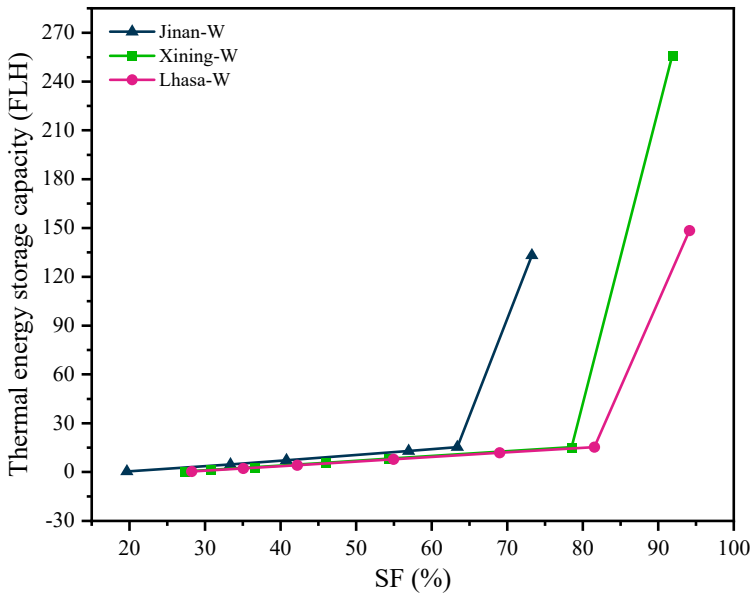

Figure 5. Relationship between thermal energy storage capacity and solar load fraction.

As shown in Figure 6, for SOL-HFMC system equipped with TES system, the SF is almost linear with the collector area, which significantly increases with the increase in solar collector area. When the solar collector area reaches Critical Area 3, the growth rate of SF is slowed down. When the solar collector area reaches Critical Area 4, the SF of three studied locations is stabilized at the maximum value of 90.7%, 92.76% and 97.34% for Jinan, Xining and Lhasa, respectively. Under the same solar collector area, regardless of whether equipped with TES system, the SF in Lhasa is the highest, followed by Xining, while the SF value in Jinan is the lowest. This is because the Lhasa region has the richest solar energy resources, and the solar collectors with the same area can collect more solar irradiation to provide energy for solvent regeneration.

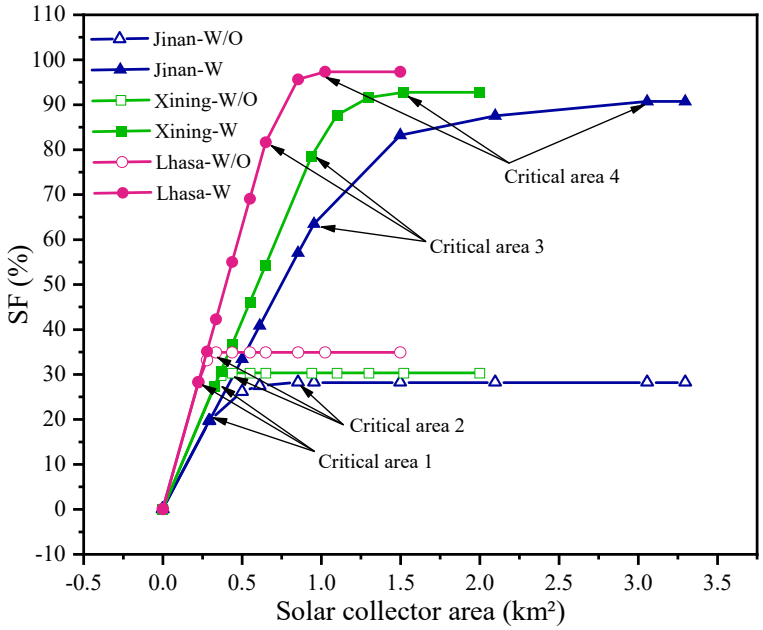

Figure 6. Relationship between SF and solar collector area.

In comparison with the STE-HFMC power plant, the work loss of gas turbine is reduced and the output capacity of the SOL-HFMC power plant is increased with the assistance of solar thermal energy for absorbent regeneration. Under the maximum SF, the differences in output capacity and net efficiency between the power plant with and without assistance of solar energy are illustrated in

 doi:10.20944/preprints202404.0550.v1

Figure 7. It can be observed that, output capacity and net efficiency of the power plant are both decreased significantly by 17% and 39% for STE-HFMC system in comparison with the baseline power plant, respectively. Compared to STE-HFMC power plant, the output capacity and net efficiency of the SOL-HFMC power plant are increased evidently, regardless whether TES system is applied or not. The most significant improvement is observed in Lhasa, followed by Xining and Jinan. Furthermore, the performance of SOL-HFMC power plant equipped with TES system is superior to that of SOL-HFMC power plant without TES system, with the net efficiency increased by 2.00%, 2.04% and 2.13% in Jinan, Xining and Lhasa, respectively. The reason can be attributed to that, TES system provides more energy for solvent regeneration and more steam can be used for power generation.

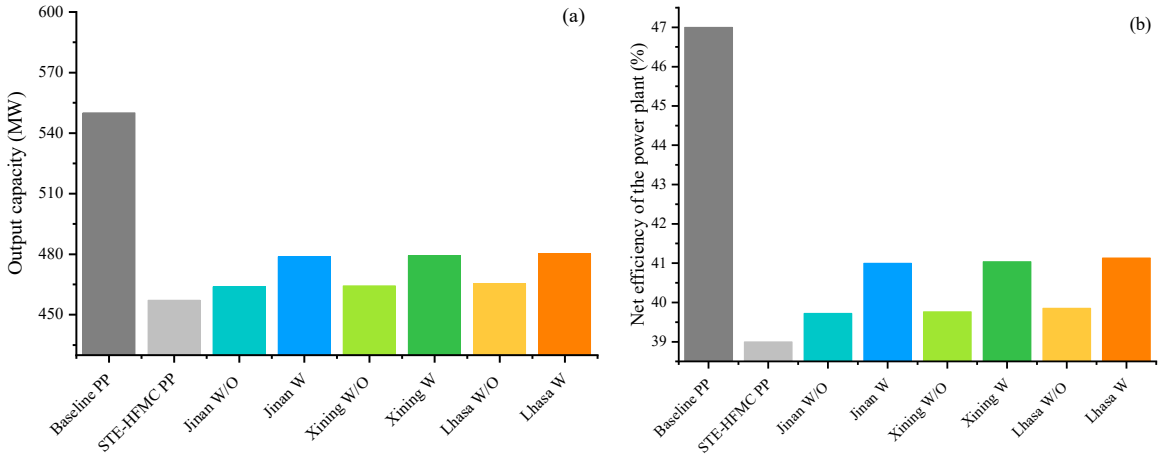

Figure 7. Output capacity and net efficiency of power plant with different configurations.

Figure 8 presents the influence of solar collector area on carbon emission intensity. The CEI value of STE-HFMC power plant is 96.50 kg CO_2/MWh. For SOL-HFMC power plant without TES system, the CEI decreases rapidly with the increase in solar collector area. The reduction rate is slowed down when the solar collector area is higher than Critical Area 1. When the solar collector area reaches Critical Area 2, the CEI value is stabilized at its minimum value of 95.10 kg CO_2/MWh, 95.00 kg CO_2/MWh and 94.78 kg CO_2/MWh for Jinan, Xining and Lhasa, respectively. Under Critical Area 2, the thermal energy provided by solar collectors reaches to its maximum value and no more extracted steam can be saved to generate more electricity in the power plant. For SOL-HFMC power plant with TES system, the CEI also decreases rapidly before the solar collector area reaches Critical Area 3 and then decreases slowly and is stabilized under Critical Area 4 at its minimum value of 92.14 kg CO_2/MWh, 92.05 kg CO_2/MWh and 91.84 CO_2/MWh for Jinan, Xining and Lhasa, respectively. For the same system under the same solar collector area, the CEI is the highest in Jinan, followed by Xining and Lhasa, because CEI strongly depends on the solar irradiation of the studied location.

Preprints.org (www.preprints.org) | NOT PEER-REVIEWED | Posted: 9 April 2024 doi:10.20944/preprints202404.0550.v1

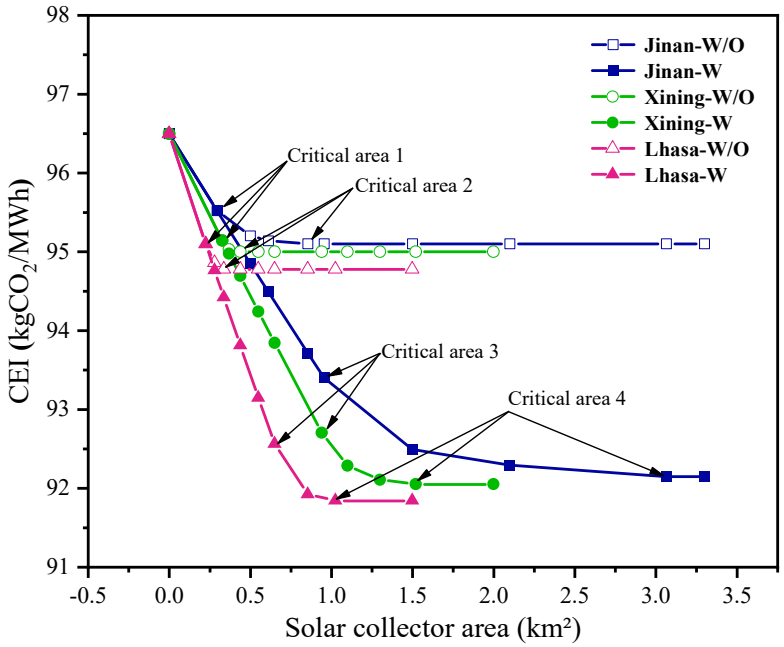

Figure 8. Change of CEI with the solar collector area.

4.2. Economic Performance Evaluation

It is obvious that the SF of SOL-HFMC power plant with TES system is relatively higher than that without TES system, leading to enhancement of output capacity of power plant. However, the introduction of TES system also results in the increase of investment costs mainly due to the cost of the phase change material. Figure 9 presents the dependence of TES system cost on the SF under the condition of maximum thermal storage capacity of 15FLH. As shown in the figure, TES system is deactivated and has no cost when the SF is lower than the SF value corresponding to Critical Area 1, which is 19.65%, 27.34% and 28.24% for Jinan, Xining and Lhasa, respectively. Then TES system is activated when the SF is higher than the point corresponding to Critical Area 1 to utilize the solar energy resources to its maximum extent, with the TES system cost linearly increases with the SF increase. When the SF reaches to the value corresponding to Critical Area 3, the TES system capacity is 15FLH and the TES cost achieves the highest. At the given value of SF, the TES system cost in Jinan City is the highest, followed by Xining and Lhasa.

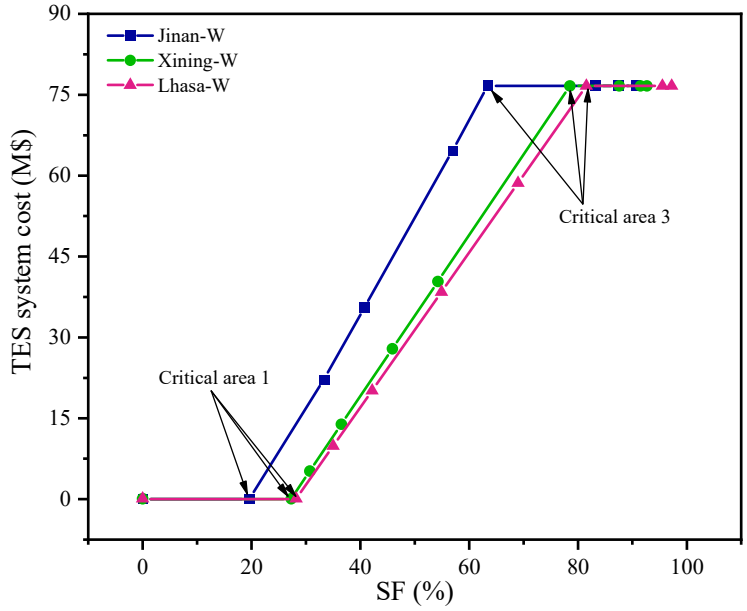

Figure 9. Dependence of TES system cost on SF.

 doi:10.20944/preprints202404.0550.v1

The total capital requirements of SOL-HFMC power plant are increased due to existence of solar thermal energy collection and storage system. LOCE and COR of the SOL-HFMC power plant with TES system are further calculated, with the results shown in Figure 10. When the area of solar collectors is zero, the LCOE and COR values of the SOL-HFMC power plant with or without TES system are the same as those of the STE-HFMC power plant, which are 91.59 $/MWh and 32.61 $/tCO$_2$, respectively.

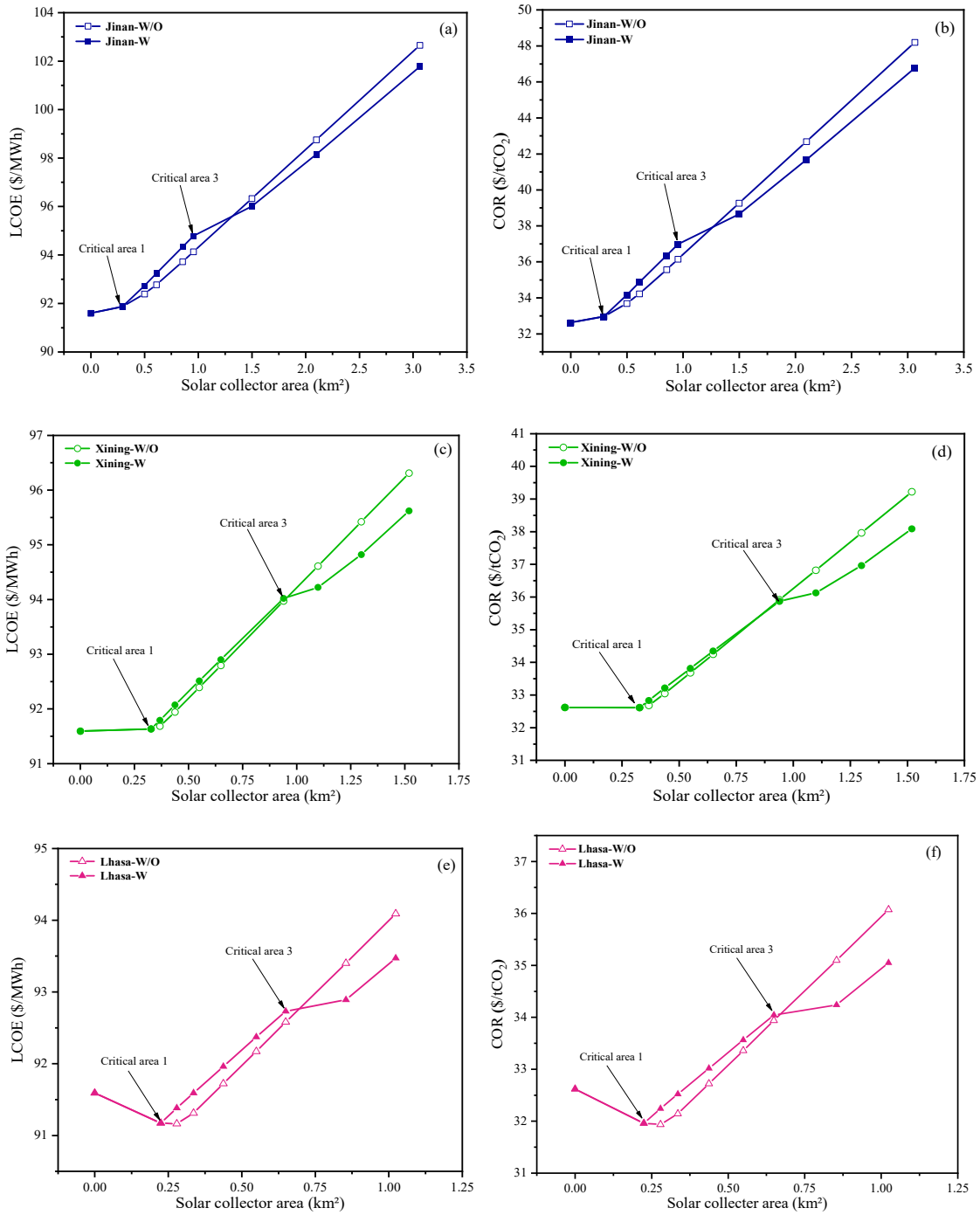

Figure 10. Variations of the LCOE and COR with solar collector area.

For SOL-HFMC power plant without TES system, the LCOE and COR values in Jinan and Xining cities both increase with the increase in solar collector area. However, in Lhasa, the LCOE and COR values show difference tendency, which decrease and then increase with the increase in solar collector area. It can be attributed to that, more steam is used for electricity generation due to higher solar irradiation intensity and longer sunshine hours in Lhasa, and thus steam saved per unit area of solar

 doi:10.20944/preprints202404.0550.v1

collector has better economic benefits than the cost increase with the introduction of solar collectors before the area reaches Critical Area 1.

For SOL-HFMC power plant with TES system, the LCOE and COR values of three studied locations are identical with the SOL-HFMC power plant without TES system when the collector area varies within the range from 0 to Critical Area 1. Within the range from Critical Area 1 to Critical Area 3, the LCOE and COR values increase rapidly with the increase in collector area, no matter what location is studied. When the collector area further exceeds Critical Area 3, the growth rate of LCOE and COR is reduced. At a given collector area, the LCOE and COR values of the SOL-HFMC power plant equipped with TES system gradually become lower than those of the plant without TES system, because the TES system cost reaches to its maximum value and no longer increases with increasing collector area. Therefore, when the solar collector area is higher than Critical Area 3, STE-HFMC power plant shall be equipped with TES system from the economic perspectives.

5. Sensitivity Analysis

5.1. Sensitivity Study on Membrane Prices

The cost of the polypropylene membrane material accounts for 64% of the total cost of hollow fiber membrane contactors [12]. Therefore, the membrane price is a critical parameter to evaluate the economic performance of SOL-HFMC power plant. Figure 11 shows the variation of the LCOE and COR values with changes of the membrane prices. The LCOE and COR values corresponding to Critical Area 2 of vacuum tube collector in a solar-assisted ammonia-based power plant in Xi'an City calculated by Liu et al.[19]are also expressed in Figure 11 as the comparison point. It can be found that, the values of LCOE and COR linearly increases when the membrane price varies within the range of 0.01-0.05 $/m in for all three studied locations.

For SOL-HFMC power plant without TES system, when the membrane price is set at 0.01 $/m, the LCOE is reduced by 2.9%, 4.7% and 5.3%, and COR is reduced by 36.1%, 40% and 42.2% compared with the reference point in Lhasa, Xining and Jinan, respectively. From the perspective of LCOE, the LCOE value is better than the value of comparison point when the membrane price is lower than 0.014 $/m, 0.017 $/m and 0.018$/m for Jinan, Xining and Lhasa cities, respectively. From the perspective of COR, the COR value is lower than the value of comparison point when the membrane price is lower than 0.032 $/m, 0.034 $/m and 0.036 $/m for Jinan, Xining and Lhasa cities, respectively.

For SOL-HFMC power plant with TES system, when the membrane price is set at 0.01 $/m, the LCOE is reduced by 1.5%, 3.9% and 4.4%, and COR is reduced by 33.7%, 39.4% and 40.7% compared with the comparison point in Lhasa, Xining and Jinan, respectively. From the perspective of LCOE, the LCOE value is superior to the value of comparison point when the membrane price is lower than 0.012 $/m, 0.015 $/m and 0.016 $/m for Jinan, Xining and Lhasa cities, respectively. From the perspective of COR, the COR value is lower than the value of comparison point when the membrane price is lower than 0.030 $/m, 0.033 $/m and 0.034 $/m for Jinan, Xining and Lhasa cities, respectively.

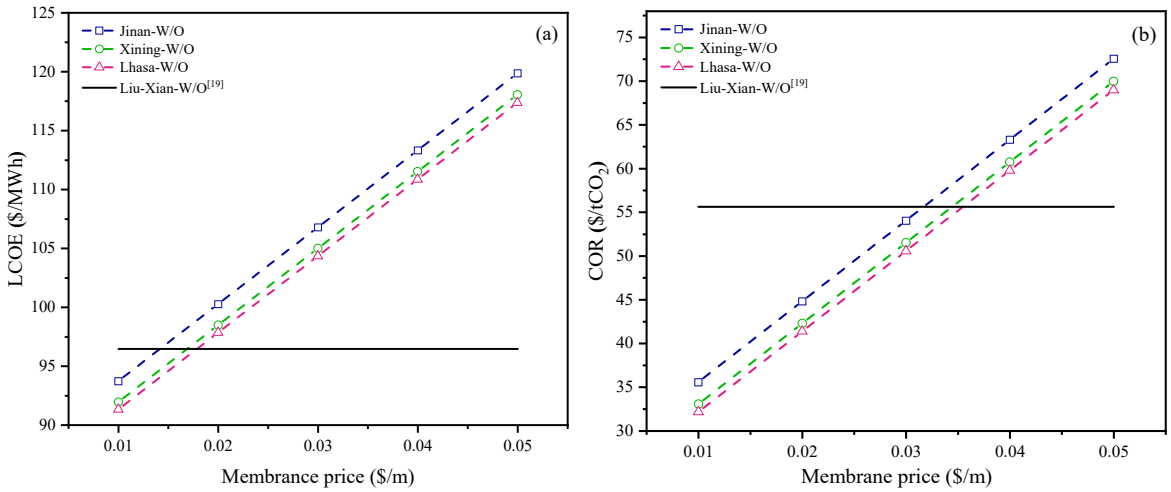

 doi:10.20944/preprints202404.0550.v1

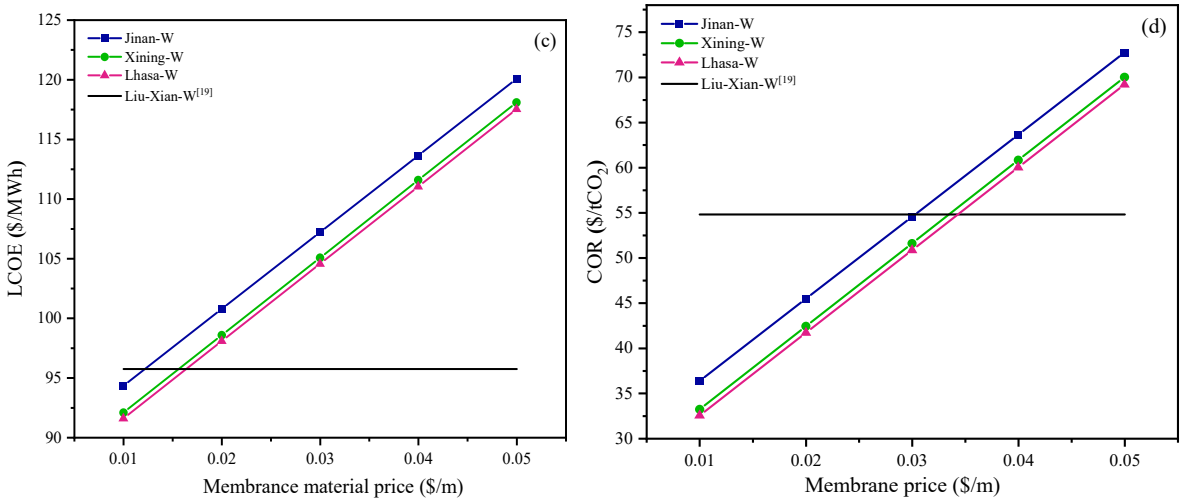

Figure 11. Variations of LCOE and COR with the membrane prices.

5.2. Sensitivity Study on Solar Collector Prices

To investigate the influence of price variation of vacuum tube collectors on the economic viability of SOL-HFMC power plant, Figure 13 presents the variations of LCOE and COR values with changes of VTC prices. For comparison, the LCOE and COR values of the STE-HFMC power plant are drawn in Figure 12. It can be clearly found that, the LCOE and COR values of the STE-HFMC power plant are fixed values which are not influenced by the price variations of vacuum tube collector, because the regeneration energy is totally supplied by the steam extracted from the gas turbine. When the price of vacuum tube collector varies in the range of 80-200 $/m², the LCOE and COR values of the SOL-HFMC power plant with or without TES system linearly increase with the increasing solar collector price for all three studied locations. At a given VTC price, the LCOE and COR value of Lhasa are lower than those of Xining, and Jinan has the highest LCOE and COR values. For the same studied location, the introduction of TES system increases the LCOE and COR values of STE-HFMC power plant under the same VTC price. To achieve better economic performance compared to the STE-HFMC power plant, if TES system is not applied, the critical VTC price is 50.1 $/m² and for Jinan, 104.7 $/m² for Xining, and 155 $/m² for Lhasa, respectively. When TES system is applied, the corresponding VTC prices shall be reduced to be lower than 25.7 $/m² and for Jinan, 95.2 $/m² for Xining, and 128.7 $/m² for Lhasa, respectively. It can be concluded that, the critical price in location with higher solar irradiation resource is higher than that of the location with poorer solar resource. Thus, it is more attractive to apply the proposed SOL-HFMC system in the power plants with rich solar resources.

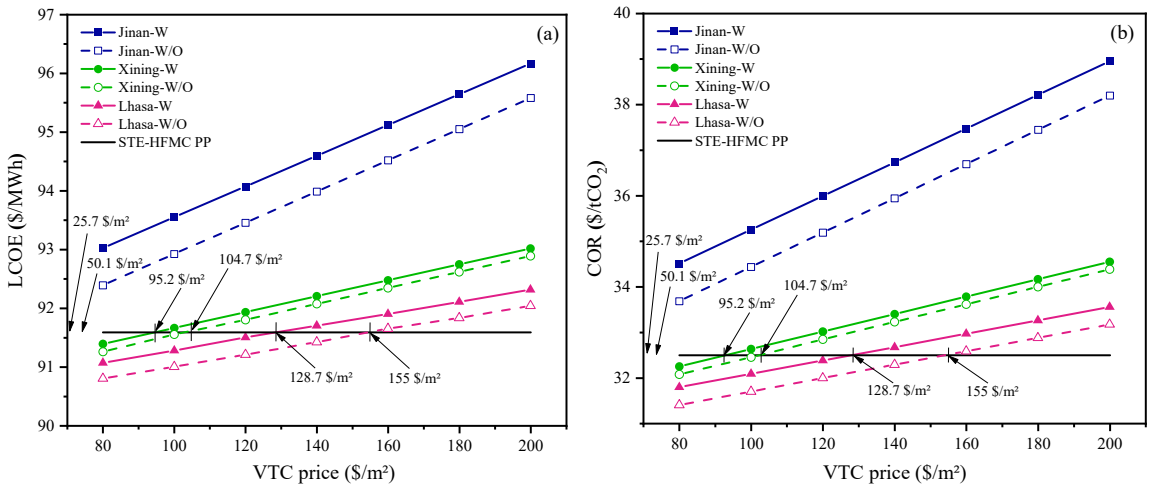

Figure 12. Variations of LCOE and COR with the VTC price.

 doi:10.20944/preprints202404.0550.v1

5.3. Sensitivity Study on PCM Prices

If TES system is integrated with SOL-HFMC power plant, the PCM prices will affect the LCOE and COR values. As shown in Figure 13, the LCOE and COR values linearly increase with the increase of the PCM price for all three studied locations. Even though the PCM price is reduced to 1.00 $/t, it cannot make the LCOE and COR values of Jinan and Xining lower than the corresponding values of the STE-HFMC power plant. However, for Lhasa city, the SOL-HFMC power plant is competitive than the STE-HFMC power plant when the PCM price is reduced to be lower than 3.53 $/t.

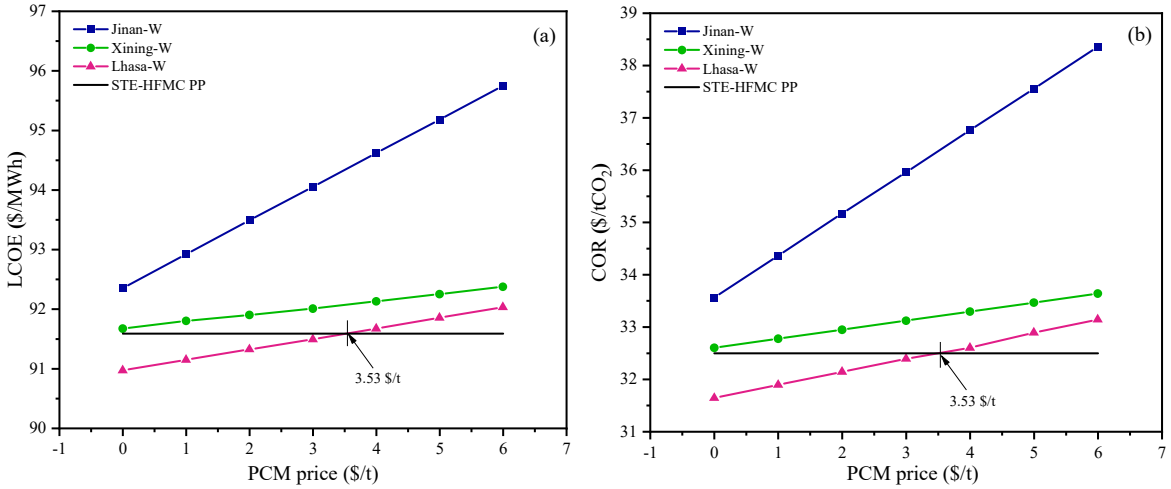

Figure 13. Variations of LCOE and COR with PCM price.

6. Conclusions

In the present paper, a novel hybridization system, which utilizes the solar thermal energy to assist with the CO_2-rich absorbent regeneration process by membrane gas absorption technology, has been proposed to capture CO_2 from the flue gas of fossil fuel power plants. Three locations with different weather conditions have been selected to evaluate the technical potential and economic feasibility of the proposed system. Based on the research results, the following conclusions can be drawn:

(1) Specific to the SF of the SOL-HFMC power plant without TES system, the SF reaches its maximum value of 28.19%, 30.26% and 34.84% when the solar collector area reaches Critical Area 2 in Jinan, Xining and Lhasa cities, respectively. If TES system is applied, the SF can reach its maximum value of 90.7%, 92.76% and 97.34% for Jinan, Xining and Lhasa, respectively. In this study, the SF value could not reach 100% due to TES capacity limitation of 15 FLH.

(2) From the perspective of technical potential, the output capacity and net efficiency of the SOL-HFMC power plant are both significantly improved in comparison with the STE-HFMC power plant, regardless of whether the TES system is equipped or not. The performance of SOL-HFMC power plant equipped with TES system is superior to that of SOL-HFMC power plant without TES system, with the net efficiency increased by 2.00%, 2.04% and 2.13% in Jinan, Xining and Lhasa, respectively.

(3) Specific to the CEI value, the minimum CEI value of the proposed SOL-HFMC power plant with TES system can be stabilized at 92.14 kg CO_2/MWh, 92.05 kg CO_2/MWh and 91.84 CO_2/MWh in Jinan, Xining and Lhasa, respectively. For SOL-HFMC power plant without TES system, the CEI value is decreased by 1.40 kg CO_2/MWh, 1.50 kg CO_2/MWh and 1.73 kg CO_2/MWh in Jinan, Xining and Lhasa, respectively, compared to 96.50 kg CO_2/MWh in STE-HFMC power plant.

(4) To achieve better economic performance compared to the STE-HFMC power plant, if TES system is not applied, the critical VTC price is 50.1 $/m^2 and for Jinan, 104.7 $/m^2 for Xining, and 155.1$/m^2 for Lhasa, respectively. When TES system is applied, the corresponding VTC prices shall be reduced to be lower than 25.7 $/m^2 for Jinan, 95.2$/m^2 for Xining, and 128.7 $/m^2 for Lhasa, respectively. For Lhasa city with rich source resources, the SOL-HFMC power plant is competitive than the STE-HFMC power plant when the PCM price is lower than 3.53 $/t.

 doi:10.20944/preprints202404.0550.v1

(5) The membrane price is also critical for the economic performance of SOL-HFMC power plant. In comparison with the reference point, for SOL-HFMC power plant with TES system, the LCOE is reduced by 1.5%, 3.9% and 4.4%, and COR is reduced by 33.7%, 39.4% and 40.7% at a given membrane price of 0.01 $/m in Lhasa, Xining and Jinan, respectively.

Author Contributions: Junkun Mu: methodology, validation, formal analysis, writing-original draft preparation; Jinpeng Bi: writing-original draft preparation, data curation, visualization, validation; Yuexia Lv: conceptualization, methodology, writing- review and editing, Supervision; Yancai Su: writing-review and editing, funding acquisition, supervision; Wei Zhao: visualization, validation, formal analysis; Hui Zhang: resources, formal analysis; Tingting Du: writing-review and editing, funding acquisition; Fuzhao Li: data curation; Hongyang Zhou: visualization. All authors have read and agreed to the published version of the manuscript.

Funding: This research was carried out with the financial support of Young Innovative Talents Introduction & Cultivation Program for Colleges and Universities of Shandong Province (Sub-title: Innovative Research Team of Advanced Energy Equipment) granted by Department of Education of Shandong Province, Natural Science Foundation of Shandong Province (No. ZR2021ME174, No. ZR2020ME178) and Shenzhen Fundamental Research Program (No. JCYJ20220530141009020).

Data Availability Statement: Data are contained within the article.

Conflicts of Interest: The authors declare that there is no conflict of interest.

References

1. Available online: https://www.ipcc.ch/sr15/. (accessed on 13 October 2023).
2. Available online: https://net0.com/blog/net-zero-countries. (accessed on 8 March 2024).
3. Available online:https://www.irena.org/publications/2022/Jul/Chinas-Route-to-Carbon-Neutrality. (accessed on 26 October 2023).
4. Ghoniem, AF. Needs, resources and climate change: Clean and efficient conversion technologies. *Prog. Energy. Combust*. 2011, *37(1)*, 15-51.
5. Goto, K.; Yogo, K.; Higashii, T. A review of efficiency penalty in a coal-fired power plant with post-combustion CO_2 capture. *Appl. Energ*. 2013, *111*, 710-720.
6. Zahedi, R.; Ayazi, M.; Aslani, A. Comparison of amine adsorbents and strong hydroxides soluble for direct air CO_2 capture by life cycle assessment method. *Environ. Technol. Inno.* 2022, *28*, 102854.
7. Li, X.L.; Zhou, X.B.; Wei, J.W.; Fan, Y.M.; Liao, L.; Wang, H.Q. Reducing the energy penalty and corrosion of carbon dioxide capture using a novel nonaqueous monoethanolamine-based biphasic solvent. *Sep. Purif. Technol*. 2021, *265*, 118481.
8. Aghel, B.; Janati, S.; Wongwises, S.; Shadloo, MS. Review on CO2 capture by blended amine solutions. *Int. J. Greenh. Gas. Con*. 2022, *119*, 103715.
9. Bravo, J.; Drapanauskaite, D.; Sarunac, N.; Romero, C.; Jesikiewicz, T.; Baltrusaitis, J. Optimization of energy requirements for CO_2 post-combustion capture process through advanced thermal integration. *Fuel* 2021, *283*, 118940.
10. Lv, Y.X.; Yu,X.H.; Tu, S.T.; Yan,J.Y.; Dahlquist, E. Experimental studies on simultaneous removal of CO_2 and SO_2 in a polypropylene hollow fiber membrane contactor. *Appl. Energ*. 2012, *97*, 283-288.
11. Belaissaoui, B.; Favre, E. Novel dense skin hollow fiber membrane contactor based process for CO_2 removal from raw biogas using water as absorbent. *Sep. Purif. Technol*. 2018, *193*, 112-126.
12. Nguyen, K.; Iliuta, I.; Bougie F. Techno-economic assessment of enzymatic CO_2 capture in hollow fiber membrane contactors with immobilized carbonic anhydrase. *Sep. Purif. Technol*. 2023, *307*, 122702.
13. Jang, M.G.; Yun, S.; Kim, J.K. Process design and economic analysis of membrane-integrated absorption processes for CO_2 capture. *J. Clean. Prod*. 2022, *368*, 133180.
14. Scholes, C.A. Membrane contactors modelled for process intensification post combustion solvent regeneration. *Int. J. Greenh. Gas. Con*. 2019, *87*, 203-210.
15. Kumar, A.; Tiwari, A.K. Solar-assisted post-combustion carbon-capturing system retrofitted with coal-fired power plant towards net-zero future: A review. *J. CO_2 Util*. 2022, *65*, 102241.

 doi:10.20944/preprints202404.0550.v1

16. Alzhrani, A.; Romero, C.E.; Baltrusaitis, J. Sustainability Assessment of a Solar Energy-Assisted Flue Gas Amine-Based CO_2 Capture Process Using Fully Dynamic Process Models. *ACS Sustainable Chem. Eng*. 2023, *11 (31)*, 11385-11398.
17. Quang, D.V.; Milani, D.; Zahra, M.A. A review of potential routes to zero and negative emission technologies via the integration of renewable energies with CO_2 capture processes. *Int. J. Greenh. Gas. Con*. 2023, *124*, 103862.
18. Mokhtar, M.; Ali, M.T.; Khalilpour, R; Abbas, A.; Shah, N; Hajaj, A.A.; Armstrong, P.; Chiesa, M.; Sgouridis, S. Solar-assisted Post-combustion Carbon Capture feasibility study. *Appl. Energ.* 2012, *92*, 668-676.
19. Liu, L.X.; Zhao, J.; Deng, S.; An, Q.S. A technical and economic study on solar-assisted ammonia-based post-combustion CO_2 capture of power plant. *Appl. Therm. Eng*. 2016, *102*, 412-422.
20. Khalilpour, R.; Milani, D.; Qadir, A.; Chiesa, M.; Abbas, A. A novel process for direct solvent regeneration via solar thermal energy for carbon capture. *Renew. Energ*. 2017, *104*, 60-75.
21. Kev, K.; Modi, N.; Milani, D.; Luu, M.T.; Nelson, S.; Manaf, N.A.; Wang, X.L.; Negnevitsky, M.; Abbas, A. A comparative life cycle impact assessment for solar heat integration in post-combustion carbon capture. *Energ. Convers. Manage*. 2023, *297*, 117745.
22. NETL, C. Performance Baseline for Fossil Energy Plants, Volume 1: Bituminous Coal and Natural Gas to Electricity, Revision 2. 2010, DOE/NETL-2010/1397.
23. Vinjarapu, S.H.B.; Regueira, T.; Neerup, R.; Solms,N.V.; Fosbøl, P.L. Heat of absorption of CO_2 in 30 wt% MEA with monoethyleneglycol and urea as vapour reduction additives. *Energy* 2024, *294*, 130609.
24. Kim, K.; Lee, H.; Park, H.S.; Song, H.; Kim, S. Surface modification of polypropylene hollow fiber membranes using fluorosilane for CO2 absorption in a gas-liquid membrane contactor. *Heliyon*. 2023, *9 (9)*, e19829.
25. Wang, Z.; Fang, M.X.; Ma, Q.H.; Zhao, Z.; Wang, T.; Luo, Z.Y. Membrane Stripping Technology for CO_2 Desorption from CO_2-rich Absorbents with Low Energy Consumption. *Energy Procedia*. 2014, *63*, 765-772.
26. Yan, Q.; Yang, Y.; Nishimura, A.; Kouzani, A.; Hu, E. Multi-point and multi-level solar integration into a conventional coal-fired power plant. *Energy Fuels*. 2010, *24*, 3733-3738.
27. Mokhta, M.; Ali, M.T.; Khalilpour, R.; Abbas, A.; Shah, N.; Hajaj, A.A.; Armstrong, P.; Chiesa, M.; Sgouridis, S. Solar-assisted post-combustion carbon capture feasibility study. *Appl. Energ*. 2012, *92*, 668-676.
28. Sweet, M.L.; McLeskeyJr, J.T. Numerical simulation of underground Seasonal Solar Thermal Energy Storage (SSTES) for a single-family dwelling using TRNSYS. *Sol. Energy* 2012, *86(1)*, 289-300.
29. Chen, J.F.; Dai, Y.J.; Wang, R.Z. Experimental and analytical study on an air-cooled single effect LiBr-H_2O absorption chiller driven by evacuated glass tube solar collector for cooling application in residential buildings. *Sol. Energy* 2017, *151*, 110-118.
30. Zhao, R.K.; Liu, L.C.; Zhao,L.; Deng, S.; Li, S,J.; Zhang, Y.; Li, H.L. Techno-economic analysis of carbon capture from a coal-fired power plant integrating solar-assisted pressure-temperature swing adsorption (PTSA). *J. Clean. Prod.* 2019, *214*, 440-451.
31. Rubin, E.S.; Short, C.; Booras, G.; Davsion, J.; Ekstrom, C.; Matuszewski, M.; McCoy, S. A proposed methodology for CO_2 capture and storage cost estimates. *Int. J. Greenh. Gas. Con*. 2013, *17*, 488-503.
32. Theis, J. Quality guidelines for energy systems studies: cost estimation methodology for NETL assessments of power plant performance. *National Energy Technology Laboratory (NETL)*. 2021.
33. Li, K.; Leigh, W.; Feron,P.; Yu, H.; Tade, M. Systematic study of aqueous monoethanolamine (MEA)-based CO_2 capture process: Techno-economic assessment of the MEA process and its improvements. *Appl. Energ*. 2016, *165*, 648-659.
34. Meteotest, J.R.; Kunz, S. MeteonormData (Worldwide).Available online: https://meteonorm.com/en/ (accessed on 11 December 2023).